Technical University of Denmark

DTU

Multivariate Analysis of Variance: Finding significant growth in mice with craniofacial dysmorphology caused by the Crouzon mutation

Thorup, Signe Strann; Ólafsdóttir, Hildur; Darvann, Tron Andre; Hermann, Nuno V.; Larsen, Per; Paulsen, Rasmus Reinhold; Perlyn, Chad A.; Morriss-Kay, Gillian M.; Kreiborg, Sven; Larsen, Rasmus

DTU Library
Technical Information Center of Denmark

Multivariate Analysis of Variance: Finding significant growth in mice with craniofacial dysmorphology caused by the Crouzon mutation

Signe Strann Thorup[a,b], Hildur Ólafsdóttir[a,b], Tron A. Darvann[b], Nuno V. Hermann[b,c], Per Larsen[b], Rasmus R. Paulsen[a,b] Chad A. Perlyn[d], Gillian M. Morriss-Kay[e], Sven Kreiborg[b,c,f], Rasmus Larsen[a]

[a] DTU Informatics, Technical University of Denmark, Lyngby, Denmark

[b] 3D Craniofacial Image Research Laboratory, School of Dentistry, University of Copenhagen; Copenhagen University Hospital and DTU Informatics, Technical University of Denmark, Lyngby, Denmark

[c] Pediatric Dentistry and Clinical Genetics, School of Dentistry, Faculty of Health Sciences, University of Copenhagen, Denmark

[d] Division of Plastic Surgery, Washington University School of Medicine, St. Louis, MO, USA

[e] Department of Physiology, Anatomy and Genetics, Oxford University, Oxford, UK

[f] Department of Clinical Genetics, The Juliane Marie Centre, Copenhagen University Hospital, Copenhagen, Denmark

INTRODUCTION:

Crouzon syndrome is characterized by growth disturbances caused by premature fusion of the cranial growth zones. A mouse model with mutation $Fgfr2^{C342Y}$, equivalent to the most common Crouzon syndrome mutation (henceforth called the Crouzon mouse model), has a phenotype showing many parallels to the human counterpart.

Quantifying growth in the Crouzon mouse model could test hypotheses of the relationship between craniosynostosis and dysmorphology, leading to better understanding of the causes of Crouzon syndrome as well as providing knowledge relevant for surgery planning.

In the present study we used micro-CT scans of 4-week-old mice (N=5) and 6-week-old mice (N=10) with Crouzon syndrome ($Fgfr2^{C342Y/+}$) were compared to control groups of 4-week-old wild-type mice (N=5) and 6-week-old wild-type mice (N=10), respectively.

MATERIAL:

The production of the $Fgfr2^{C342Y/+}$ mutant mouse (Crouzon mouse) was carried out as described by Eswarakumar et al. (2004). All procedures were in agreement with the United Kingdom Animals (Scientific Procedures) Act, guidelines of the Home Office, and regulations of the University of Oxford.

Before micro-CT scanning, the mice were euthanized by CO_2 asphyxiation and whole mount skeletal preparations were carried out. 3D volumes of the skull of size 720×480×480 voxels were obtained at approximately $46\mu m \times 46\mu m \times 46\mu m$ resolution per voxel using a General Electric Medical Systems EVS-RS9 Micro-CT scanner.

Prior to processing the images, the neck part was removed from all 30 images since the mice were decapitated at different positions prior to scanning. The hyoid bone was also removed due to its random position and scanning artefacts. Due to the large variation the Crouzon mice, these mice were mirrored to get the nose deviate to the same side.

METHODS:

As a common reference frame, a 3D mean shape (atlas) was created for the 6-week wild-type mice using automatic non-rigid volumetric image registration based on B-splines ([1,2]). All mice were then registered to the atlas using a rigid transformation [3] for alignment (no scaling was allowed because knowledge about growth is important in this study) and afterwards non-rigid image registration was applied to get all the local changes. From the non-rigid registration a dense field of deformation

vectors was extracted for each mouse-type and due to the choice of reference all mice got point correspondence.

Average growth was quantified using atlases created for each of the four mouse-groups. By extracting the deformation vectors (growth) between 4- and 6-week mice for each type, the average growth could be visualised.

Due to the cross-sectional data, a multivariate analysis of variance (MANOVA) was carried out on the deformation vectors in order to evaluate the statistical significance of growth. The objective was to identify whether changes in the independent variables had a significant effect on the dependent variables as well as to indentify the possible interactions among the independent variables and the connection among dependent variables. By splitting the dataset into four groups depending on age and mouse-type, it was possible to test whether the group means are different and determine spatial location of any significant differences.

Given that the data is mutually independent, identically distributed (same probability function) and Gaussian, a model can be set up. Let $\mathbf{a}$ denote the mouse-type, $\mathbf{b}$ the age and $\mathbf{ab}$ the interaction between age and mouse-type. It is then assumed that every observation can be written as

$$\boldsymbol{X}_{ijv} = \begin{bmatrix} x_{ijv} \\ y_{ijv} \\ z_{ijv} \end{bmatrix} \text{ with } i = 1,2 \text{ or } \{\text{normal, Crouzon}\}, j = 1,2 \text{ or } \{\text{4-week, 6-week}\} \text{ and } v = \{1,2,...,n_{ij}\} \text{ or}$$

repetitions (number of mice in each group, which is five or ten), and we set up the model:

$$\boldsymbol{X}_{ijv} = \boldsymbol{\mu} + \boldsymbol{a}_i + \boldsymbol{b}_j + \boldsymbol{ab}_{ij} + \boldsymbol{\epsilon}_{v(ij)},$$
$$\sum \boldsymbol{a}_i = 0, \sum \boldsymbol{b}_j = 0, \sum_i \boldsymbol{ab}_{ij} = \sum_j \boldsymbol{ab}_{ij} = 0.$$

Table 1 shows the scheme for carrying out the MANOVA.

| E{ }	B₁ (4-week)	B₂ (6-week)
A₁ (Wild-type mice)	$\boldsymbol{\mu} - \boldsymbol{a} - \boldsymbol{b} - \boldsymbol{ab}$	$\boldsymbol{\mu} - \boldsymbol{a} + \boldsymbol{b} + \boldsymbol{ab}$
A₂ (Crouzon mice)	$\boldsymbol{\mu} + \boldsymbol{a} - \boldsymbol{b} + \boldsymbol{ab}$	$\boldsymbol{\mu} + \boldsymbol{a} + \boldsymbol{b} - \boldsymbol{ab}$

Table 1 - Expected mean values found with the model in equation 1. The idea is that every mouse can be constructed as an overall mean plus/minus age, mouse-type and interaction between age and type.

Table 2 shows the table for carrying out the MANOVA on the mouse data.

	B₁ (4-week)	B₂ (6-week)	
A₁ (Wild-type mice)	$\bar{\boldsymbol{X}}_{11.}$ n_{11}	$\bar{\boldsymbol{X}}_{12.}$ n_{12}	$\bar{\boldsymbol{X}}_{1..}$ $n_{11}+n_{12}$
A₂ (Crouzon mice)	$\bar{\boldsymbol{X}}_{21.}$ n_{21}	$\bar{\boldsymbol{X}}_{22.}$ n_{22}	$\bar{\boldsymbol{X}}_{2..}$ $n_{21}+n_{22}$
	$\bar{\boldsymbol{X}}_{.1.}$ $n_{11}+n_{21}$	$\bar{\boldsymbol{X}}_{.2.}$ $n_{12}+n_{22}$	$\bar{\boldsymbol{X}}_{...}$ $n_{11}+n_{12}+n_{21}+n_{22}$

Table 2 - Table for MANOVA testing. $\bar{X}_{11.}$ is the mean of the 4 week normal mice with n_{11} number of mice, similar for $\bar{X}_{12.}, \bar{X}_{21.}, \bar{X}_{22.}$. $\bar{X}_{1..}$ is the sum of the two means in the A₁ row, $\bar{X}_{.1.}$ is the sum of the two means in the B₁ column, similar for $\bar{X}_{2..}$ and $\bar{X}_{.2.}$. $\bar{X}_{...}$ is the sum of the means $\bar{X}_{11.}, \bar{X}_{12.}, \bar{X}_{21.}$ and $\bar{X}_{22.}$. The n's are the number of mice in each group with $n_{11} = n_{21} = 5$ and $n_{12} = n_{22} = 10$ in this study.

RESULTS AND DISCUSSION:
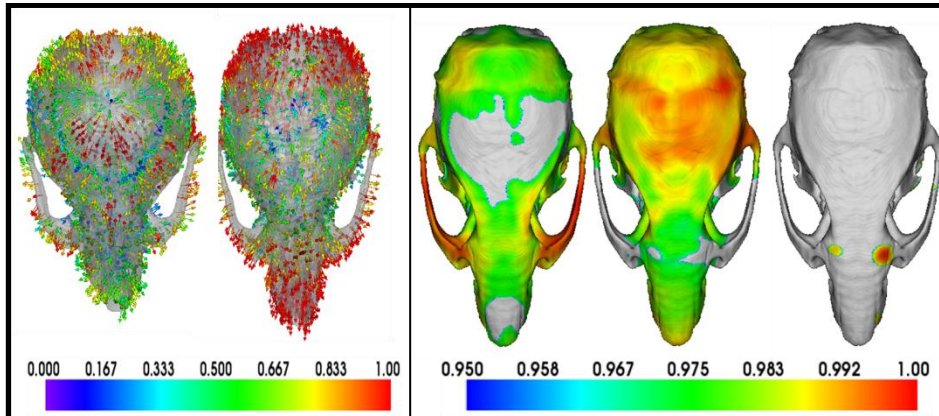
Figure 1 – Left box: From left to right Crouzon and wild-type, respectively. Deformation vectors are shown on the 4-week atlases. The colours denote displacement with respect to atlas (in mm), with red denoting most change and blue smallest change. **Right box:** Significant areas shown on 6-week normal atlases. From left to right the images show significant areas with respect to age, mouse-type and interaction between age and mouse-type. Non-significant areas are grey and significant areas are rated from blue (least significant) to red (very significant). The colours are intended to enhance the differences. All three variables were tested at a 95% level using an F-test.

Visualisations of the average growth for Crouzon mice showed growth inhibition in the front (nose, front of calvaria) and in the back (posterior part of calvaria) of the skull, see Figure 1. However, the vertical, downwards growth seemed to be similar in the two groups. Seen from the side, the nose in the normal mice elevated and extended forwards because of the growth in the sutures - in the Crouzon mice the nose did not elevate at all (and extended by a very small amount). This is probably the effect of fused sutures. Although the nose did not extend much, and did not elevate, the orbital rims extended forward by a large amount; it also elevated slightly at the anterior end, creating a pronounced bulge between the eyes. The bulge was not present at 4 weeks, but became very pronounced at 6 weeks. The mandible did not move as much forward in Crouzon mice as in the normal mice. The posterior edge of the mandible stayed in the same place relative to the ear/posterior part of calvaria, while in the normal mice this distance increased: the posterior part lifted and extended like the front of the mouse. Notice, that the growth observed depends on the chosen alignment of the mice. In this study the growth is a result of the mathematical alignment from the image registration i.e. the mice are aligned in the area near the posterior part of the orbital rim.

The MANOVA showed very significant growth in the orbital rims and mandible, and significant growth in the posterior part of the skull, tip of the nose and the section of the nose near the eyes. Because of the construction of the MANOVA, these areas show where the growth is similar for 4- and 6-week old mice – i.e. we are comparing the mean of 4-weeks to the 6-weeks independent of type. Regarding the results for significant differences related to type, very significant differences seems to relate to the larger height and widening of the skull in Crouzon mice, and the significant changes also occur for the posterior part of the skull and nose region.

The interaction between type and age showed few significant areas but is as such zero. The two dots on the nose are probably the bulges seen in the visualisations of the Crouzon mice. As previously stated these became more pronounced from 4 to 6 weeks.

Age, type and interaction were all tested using an *F*-test with a 95% level.

The registrations were qualitatively validated through visualization of the deformation secondly quantitatively validated using expert-placed landmarks.

CONCLUSION:

Image registrations made it possible to automatically quantify and visualise average craniofacial growth in normal and Crouzon mouse models, and significantly different growth patterns were found between the two.

The visualised deformation vectors proved growth in the Crouzon group to be inhibited, especially in the nasal and posterior regions of the skull compared to the growth in the normal group, and showed an expansion vertically and laterally in the middle and anterior part of the calvaria.
With the MANOVA, we were able to separate the growth vectors from the visualisations into three classes; age, type, and interaction between type and age. But overall we got a similar result to the visualised deformations.

The methodology generalises to quantification of shape and growth in other mouse models, and provides a tool for spatially detailed automatic phenotyping.

REFERENCES:

[1]   D. Rueckert, L. I. Sonoda, C. Hayes, D. L. G. Hill, M. O. Leach, and D. J. Hawkes. Non- rigid registration using free-form deformations: Application to breast MR images. IEEE Transactions on Medical Imaging, 18(8):712-721, 1999.

[2]   J. A. Schnabel, D. Rueckert, M. Quist, J. M. Blackall, A. D. Castellano Smith, T. Hartkens, G. P. Penney, W. A. Hall, H. Liu, C. L. Truwit, F. A. Gerritsen, D. L. G. Hill, and D. J. Hawkes. A generic framework for non-rigid registration based on non-uniform multi-level free-form deformations. In Fourth Int. Conf. on Medical Image Computing and Computer- Assisted Intervention (MICCAI '01), pages 573-581, Utrecht, NL, October 2001.

[3]   C. Studholme, D.L.G.Hill, D.J. Hawkes, An Overlap Invariant Entropy Measure of 3D Medical Image Alignment, Pattern Recognition, Vol. 32(1), Jan 1999, pp 71-86.